

## **EFFICIENT APPROACH FOR SENSITIVITY ANALYSIS OF LOSSY AND LEAKY STRUCTURES USING FDTD**

**M. A. Swillam**

Department of Electrical and Computer Engineering  
McMaster University  
Hamilton, Ontario L8S 4K1, Canada

**R. H. Gohary**

Communications Research Centre  
Ottawa, Ontario K2H 8S2, Canada

**M. H. Bakr and X. Li**

Department of Electrical and Computer Engineering  
McMaster University  
Hamilton, Ontario L8S 4K1, Canada

**Abstract**—An efficient approach is utilized for extracting the modal parameters of high frequency structures and their sensitivities with respect to all the design parameters. Using one FDTD simulation, the modal parameters of all the guided and leaky modes are extracted over the frequency band of interest. An adapted version of the matrix pencil method is utilized for efficient extraction of the modal parameters. In addition, using no extra simulations, the sensitivities of the propagation constants with respect to all the design parameters of the structure are extracted regardless of their number. The computational time is a small fraction of the cost of similar approaches.

### **1. INTRODUCTION**

Efficient extraction of the modal parameters of electromagnetic structures is considered as an essential step for accurate modeling [1–6]. Studying the dispersion characteristics of any structure and the impact of the design parameters on these characteristics is also

---

Corresponding author: M. A. Swillam (swillama@mcmaster.ca).

desired. The design parameters can be utilized to achieve the required dispersion characteristics as shown in [3]. In addition, the modal parameters can be utilized for calculating key design parameters such as the coupling length of microstrip and optical directional couplers [7]. It is also utilized to obtain the imaging length of multimode interference devices with different index profiles [8]. The beating length of polarization converters is determined using the modal parameters [9]. These modal parameters are also incorporated in the mode matching technique for modeling microwave and optical structures with multiple discontinuities [10]. Obtaining the sensitivities of the modal parameters or the dispersion characteristics with respect to all the design parameters is thus of prime importance. This sensitivity information is essential for tolerance and yield analysis of different devices. It also enables efficient gradient-based optimization of the behavior of these characteristics.

In the last two decades accurate calculation of the dispersion characteristics using different numerical techniques attracted numerous attentions. These numerical methods include finite difference time domain (FDTD) [1], the transmission line method (TLM) [2], the method of lines [3], and the finite difference frequency domain (FDFD) method [4]. None of these techniques, however, propose a specific approach to efficiently estimate the sensitivities of the dispersion characteristics with respect to the design parameters. The classical finite difference approximations are mainly utilized for this purpose. This technique, however, is inefficient and requires many extra simulation especially for a large number of design parameters. For example, the central finite difference approximation (CFD) requires  $2N$  additional simulations to obtain the sensitivities for a structure with  $N$  design parameters. This computational cost of the sensitivity calculations motivates research for alternative approaches.

Recently, an efficient approach for sensitivity calculations of the dispersion characteristics has been introduced [11]. This technique requires one FDTD simulation to obtain the propagation constants and their sensitivities with respect to all the design parameters for all the guided modes over the desired frequency band. The computational efficiency of this approach has been demonstrated for different lossless structures. This approach consists of two main parts. The first part extracts the modal parameters efficiently using only one FDTD simulation. The second part calculates the sensitivities of the propagation constants with respect to all the design parameters using the same simulation. Similar sensitivity analysis approaches have been recently utilized with the FDTD method for efficient design of microwave and optical components [12–14].

In the first part of the technique described in [11], the fast Fourier transform (FFT) is utilized for the extraction of the propagation constants. This technique, however, is not suitable for obtaining the modal losses. In addition, the accuracy of the obtained results is mainly governed by the number of samples in the propagation directions. This in turn increases the computational cost of the FDTD simulation.

In this paper, we propose a modified approach to obtain the modal parameters and their sensitivities using only one FDTD simulation. We utilize the matrix pencil method (MPM) for extracting the modal parameters. This method is not only capable of extracting the complex propagation constants but it also requires fewer data samples. As a result, the propagation length of the structure can be significantly shortened. This reduces the computation cost of the FDTD simulation dramatically. Using this approach, the computational time is only a small fraction of that reported in [11]. This significant reduction in the computational cost makes it possible to apply this technique for a wide range of applications in both microwave and optical frequency regimes.

We start by briefly describing the approach for efficient extraction of the propagation constants in Section 2. In Section 3, the MPM adapted for efficient extraction of the propagation constants is described. The efficient sensitivity extraction approach of the propagation constants is given in Section 4. The numerical validation examples are given in Section 5. Finally, we give our conclusion in Section 6.

## 2. MODAL PARAMETERS EXTRACTIONS

In this Section, we briefly describe the proposed technique for extracting the modal parameters of all the guided and leaky modes inside the electromagnetic structure over the desired frequency band using only one FDTD simulation. The FDTD method is one of the well known techniques in computational electrodynamics. It has been applied to the modeling of many high frequency structures, see for example [15–26].

Our derivation follows a similar approach to that in [11]. We start by decomposing the input excitation of the FDTD simulation into guided and leaky modes of the structures as follows:

$$\psi_{inp} = \psi(x, y, 0) = \sum_{m=0}^M a_m^i \Phi_m^i(x, y) \quad (1)$$

where  $\Phi_m^i(x, y)$  is the modal field of the  $m$ th mode of the structure

at frequency  $f_i$ , and  $a_m^i$  is the coefficient of the  $m$ th mode.  $M$  in (1) is the number of modes supported by the structure. After a specific propagation distance  $z$ , the harmonic field at a specific frequency  $f_i$  can be calculated as follows:

$$\tilde{\psi}_t^i(x, y, z) = \sum_m a_m^i \Phi_m^i(x, y) e^{-\gamma_m^i z} \quad (2)$$

where  $\gamma_m^i$  is the propagation constant of the  $m$ th mode at frequency  $f_i$  and is given by:

$$\gamma_m^i = \alpha_m^i + j\beta_m^i. \quad (3)$$

$\beta_m^i$  and  $\alpha_m^i$  are the phase and the attenuation terms of the propagation constant  $\gamma_m^i$ , respectively.

We define an auxiliary function in the frequency domain [27]:

$$\tilde{P}^i(z) = \iint_{\Omega} \psi_{inp}^H \tilde{\psi}_t^i(x, y, z) dx dy = \sum_m c_m^i e^{-\gamma_m^i z} \quad (4)$$

where

$$c_m^i = |a_m^i|^2 \iint_{\Omega} \Phi_m^{iH} \Phi_m^i dx dy \quad (5)$$

and  $\Phi_m^{iH}$  is the Hermitian of the  $m$ th modal field. In (4) and (5)  $\Omega$  is the cross sectional area. The complex propagation constants can be obtained from (4) using different approaches. These approaches include curve fitting techniques in the  $z$ -domain such as Prony's method [28]. They can also include smart digital signal processing approaches such as the matrix pencil method [29, 30]. For propagation constants with negligible attenuation, the FFT can be utilized as in [11]. However, this technique requires many samples in the propagation directions which increase the total simulation time.

### 3. THE MATRIX PENCIL METHOD

In this section, we use the matrix pencil method developed in [29] for efficient extraction of the propagation constants. This method has been originally developed for high resolution spectral estimation.

Here, we aim at obtaining the complex propagation constant  $\gamma_m^i$  for each mode and the amount of power coupled to this mode through the coefficients  $c_m^i$ . For this purpose, we first assume that the sequence of  $\tilde{P}^i(z)$  given by (4) is readily available from the FDTD simulation.

We also assume that the obtained sequence is contaminated with numerical noise  $v(z)$ , i.e.,

$$y^i(z) = \tilde{P}^i(z) + v(z) \tag{6}$$

Using (4), we can rewrite (6) as:

$$y_n^i = \sum_{m=1}^M c_m^i w_{i,m}^n + v_n \tag{7}$$

where  $w_{i,m}^n = e^{-\gamma_m^i(n\delta z)}$ ,  $v_n = v(n\delta z)$ ,  $y_n^i = y^i(n\delta z)$ , and  $\delta z$  is the sampling interval in the  $z$  direction. This sample interval is an integer multiple of the step size  $\Delta z$  used in the FDTD simulation.

Suppose we have  $N$  samples and the number of modes  $M$  is known, then we can construct the  $(N - M) \times M$  matrices  $\mathbf{Y}_1^i$  and  $\mathbf{Y}_2^i$  given by [29]:

$$\begin{aligned} \mathbf{Y}_1^i &= \begin{bmatrix} y_0^i & y_1^i & \cdots & y_{M-1}^i \\ y_1^i & y_2^i & \cdots & y_M^i \\ \vdots & \vdots & \vdots & \vdots \\ y_{N-M-1}^i & y_{N-M}^i & \cdots & y_{N-2}^i \end{bmatrix}, \text{ and} \\ \mathbf{Y}_2^i &= \begin{bmatrix} y_1^i & y_2^i & \cdots & y_M^i \\ y_2^i & y_3^i & \cdots & y_{M+1}^i \\ \vdots & \vdots & \vdots & \vdots \\ y_{N-M}^i & y_{N-M+1}^i & \cdots & y_{N-1}^i \end{bmatrix} \end{aligned} \tag{8}$$

By defining

$$\begin{aligned} \mathbf{W}_1^i &= \begin{bmatrix} 1 & 1 & \cdots & 1 \\ w_{i,1} & w_{i,2} & \cdots & w_{i,M} \\ \vdots & \vdots & \vdots & \vdots \\ w_{i,1}^{N-M-1} & w_{i,2}^{N-M-1} & \cdots & w_{i,M}^{N-M-1} \end{bmatrix}, \text{ and} \\ \mathbf{W}_2^i &= \begin{bmatrix} 1 & 1 & \cdots & 1 \\ w_{i,1} & w_{i,2} & \cdots & w_{i,M} \\ \vdots & \vdots & \vdots & \vdots \\ w_{i,1}^{M-1} & w_{i,2}^{M-1} & \cdots & w_{i,M}^{M-1} \end{bmatrix}, \end{aligned} \tag{9}$$

we can write

$$\mathbf{Y}_1^i = \mathbf{W}_1^i \mathbf{C}^i \mathbf{W}_2^i + \mathbf{V}_1 \quad \text{and} \quad \mathbf{Y}_2^i = \mathbf{W}_1^i \mathbf{C}^i \mathbf{W}_o^i \mathbf{W}_2^{iT} + \mathbf{V}_2 \tag{10}$$

where  $\mathbf{C}^i = \text{diag}(c_1^i, \dots, c_M^i)$ ,  $\mathbf{W}_o^i = \text{diag}(w_{i,1}, \dots, w_{i,M})$ , and the noise matrices are given by

$$\mathbf{V}_1 = \begin{bmatrix} v_o & v_1 & \dots & v_{M-1} \\ v_1 & v_2 & \dots & v_M \\ \vdots & \vdots & \vdots & \vdots \\ v_{N-M-1} & v_{N-M} & \dots & v_{N-2} \end{bmatrix}, \text{ and}$$

$$\mathbf{V}_2 = \begin{bmatrix} v_1 & v_2 & \dots & v_M \\ v_2 & v_3 & \dots & v_{M+1} \\ \vdots & \vdots & \vdots & \vdots \\ v_{N-M} & v_{N-M+1} & \dots & v_{N-1} \end{bmatrix} \quad (11)$$

For the noiseless case, one can show that the generalized eigenvalue of the matrix pencil  $(\mathbf{Y}_2^i, \mathbf{Y}_1^i)$  [29] is equal to  $w_{i,k}$ . In the noisy case this does not hold in general. However, when the numerical noise is relatively small, the generalized eigenvalues of  $(\mathbf{Y}_2^i, \mathbf{Y}_1^i)$  provide a good approximation of  $w_{i,k}$ .

From (9) it can be seen that the exponent in each row in the matrices  $\mathbf{W}_1^i$  and  $\mathbf{W}_2^i$  increases linearly with the order of the sample. In our particular application where  $\gamma_m^i$  is complex, the rows which have high order  $n$  will approach zero. On the other hand, the first row contains only ones. Hence, using a large number of data samples to construct the matrices  $\mathbf{Y}_1^i$  and  $\mathbf{Y}_2^i$  results in an ill-conditioned pencil  $(\mathbf{Y}_2^i, \mathbf{Y}_1^i)$ . This suggests that, from a practical perspective, using a moderate number of samples is recommended.

To avoid potential sources of further ill-conditioning, we should guarantee that the rows of  $\mathbf{Y}_1^i$  and  $\mathbf{Y}_2^i$  are linearly independent. In the noiseless case, the value of  $P(n\delta z)$  can be utilized at each propagation step, i.e.,  $\delta z = \Delta z$ . However, due to the smooth variation in  $P(z)$  in the presence of the numerical noise, the data at some  $\Delta z$  can be close to being linearly dependent. In order to avoid this dependence, we propose to choose  $\delta z$  as a multiple of  $\Delta z$ . In particular, we propose to choose  $\delta z$  such that  $1/\delta z$  is close to the Nyquist rate of the sequence  $P(z)$  [31]. That is, close to twice the maximum frequency of the sequence  $P(z)$ .

#### 4. SENSITIVITY ANALYSIS OF THE PROPAGATION CONSTANTS

Once the propagation constants and the coupling coefficients of all the modes over the desired bandwidth have been calculated as described in Section 3, the sensitivities of the modal characteristics can be estimated by following a similar approach to the one shown in [11]. Here, we briefly describe this approach.

We start by differentiating (4) with respect to the  $k$ th design parameter  $p_k$  at a propagation distance  $z_1$  to obtain

$$\frac{\partial \tilde{P}^i(z_1)}{\partial p_k} = \sum_{m=1}^M \frac{\partial c_m^i}{\partial p_k} e^{-\gamma_m^i z_1} - z_1 c_m^i e^{-\gamma_m^i z_1} \cdot \frac{\partial \gamma_m^i}{\partial p_k} \quad (12)$$

By evaluating the sensitivities of the auxiliary function at different propagation steps ( $z_1, \dots, z_K$ ), the following system of equations can be constructed:

$$\mathbf{Ax} = \mathbf{b} \quad (13)$$

where

$$\mathbf{A} = \begin{bmatrix} e^{-\gamma_1^i z_1} & \dots & e^{-\gamma_M^i z_1} & -z_1 c_1^i e^{-\gamma_1^i z_1} & \dots & -z_1 c_M^i e^{-\gamma_M^i z_1} \\ \vdots & \dots & \vdots & \vdots & \dots & \vdots \\ e^{-\gamma_1^i z_K} & \dots & e^{-\gamma_M^i z_K} & -z_K c_1^i e^{-\gamma_1^i z_K} & \dots & -z_K c_M^i e^{-\gamma_M^i z_K} \end{bmatrix}$$

$$\mathbf{x} = \left[ \frac{\partial c_1^i}{\partial p_k} \quad \dots \quad \frac{\partial c_M^i}{\partial p_k} \quad \frac{\partial \gamma_1^i}{\partial p_k} \quad \dots \quad \frac{\partial \gamma_M^i}{\partial p_k} \right]^T, \text{ and} \quad (14)$$

$$\mathbf{b} = \left[ \frac{\partial \tilde{P}^i(z_1)}{\partial p_k} \quad \dots \quad \frac{\partial \tilde{P}^i(z_K)}{\partial p_k} \right]^T$$

As described in [11], the vector  $\mathbf{b}$  can be obtained using the adjoint variable method (AVM) [12] which allows for efficient estimation of the derivatives of the auxiliary function  $\tilde{P}^i(z_k)$  with respect to all the design parameters without any extra simulations. Once  $\mathbf{b}$  is calculated, the sensitivities of the propagation constants and coefficients  $\mathbf{x}$  can be obtained by solving (13).

## 5. NUMERICAL EXAMPLES

In order to illustrate our approach three examples are given. In these examples, a uniaxial perfectly matched layer is utilized to terminate the computational domain [32].

### 5.1. Single Dielectric Post Loaded Waveguide

The first example is a single post partially loaded dielectric waveguide as shown in Fig. 1. The dimensions of the structure are  $a = 10.16$  mm,  $b = 5.588$  mm,  $W = 5.08$  mm, and  $L = 3.048$  mm. The length of the structure is 40.0 mm. The constitutive parameters are  $\varepsilon_{r1} = 1$ ,  $\sigma_1 = 0$ ,  $\varepsilon_{r2} = 8.0$ , and  $\sigma_2 = 0.1$  S/m. We utilize our approach to extract the complex propagation constants of all the modes over the required bandwidth. The results obtained for the fundamental TE

mode using our method and those obtained using Ansoft-HFSS [33] are shown in Figs. 2 and 3. Very good agreement is obtained between the two techniques. The modal field distribution of the fundamental mode at 19 GHz is also shown in Fig. 4.

The phase constants obtained using our approach and shown in Fig. 3 have a very good agreement with the ones obtained using the approach given [11]. However, the total computational time of our approach including the post processing of the MPM represents only 9% of the total computational time reported in [11]. This significant saving is mainly due to the utilization of MPM which requires less number of samples. This in turn reduces the length of the structure in the  $z$  directions to a small fraction of its length for the former approach.

For this example, we also extract the sensitivity of these constants with respect to all the design parameters. The vector of design parameters is  $\mathbf{p} = [a \ b \ L \ W \ \epsilon_{r1} \ \sigma_1 \ \epsilon_{r2} \ \sigma_2]^T$ . Due to space

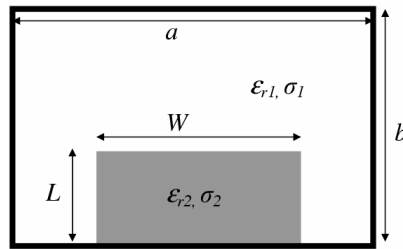


**Figure 1.** Schematic diagram of the single post loaded dielectric waveguide.

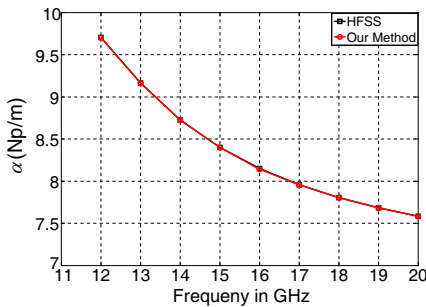


**Figure 2.** The attenuation coefficients of the dominant mode for the single post partially loaded dielectric waveguide.

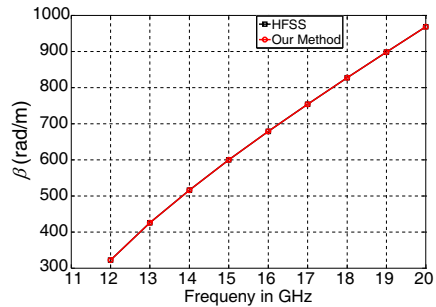


**Figure 3.** The phase constants of the dominant mode of the single post partially loaded waveguide.

limitation, we show only a part of these results. The sensitivity of the attenuation coefficient  $\alpha$  of the fundamental TE mode with respect to the permittivity of the loaded region  $\varepsilon_{r2}$  and the conductivity of the loaded region  $\sigma_2$  and its permittivity  $\varepsilon_{r2}$  are shown in Figs. 5 and 6, respectively. The results obtained using our approach are compared to those obtained using the CFD. Good match is obtained between both approaches. Using the CFD, 16 extra simulations are required. However, using our approach no extra simulation is required.

## 5.2. Double Post Dielectric Loaded Waveguide

In this example, a double post dielectric loaded waveguide shown in Fig. 7 is analyzed using our approach. The dimensions of the structure are  $a = 20.0$  mm,  $b = 11.0$  mm,  $W_1 = 5.0$  mm,  $L_1 = 3.00$  mm,  $W_2 = 5.0$  mm, and  $L_2 = 3.0$  mm. The constitutive parameters are  $\varepsilon_{r1} = 1$ ,  $\sigma_1 = 0$ ,  $\varepsilon_{r2} = 8.0$ ,  $\sigma_2 = 0.1$  S/m,  $\varepsilon_{r3} = 6.0$ , and  $\sigma_3 = 0.5$  S/m. The length of the structure is taken to be 40.0 mm. The dispersion characteristics of the fundamental TE mode over a frequency band from 10 GHz to 20 GHz are obtained using our approach and compared with the HFSS results as shown in Figs. 8 and 9.

The sensitivity of the propagation constant with respect to all the design parameters is also obtained using our approach. The vector of

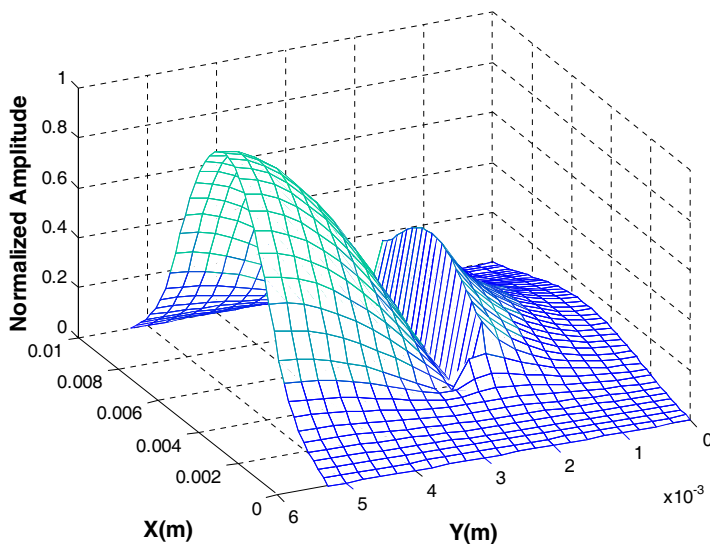


**Figure 4.** The modal field profile of the fundamental mode of the single post partially loaded waveguide calculated at 19 GHz.

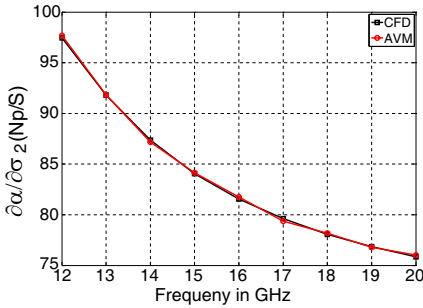


**Figure 5.** Sensitivity of the dominant mode attenuation coefficient for the single post partially loaded dielectric waveguide with respect to the conductivity  $\sigma_2$ .

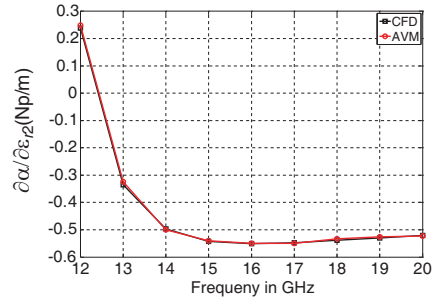


**Figure 6.** Sensitivity of the dominant mode attenuation coefficient for the single post partially loaded dielectric waveguide with respect to the permittivity  $\epsilon_{r2}$ .

the design parameters is  $\mathbf{p} = [a \ b \ L_1 \ W_1 \ L_2 \ W_2 \ \epsilon_{r1} \ \sigma_1 \ \epsilon_{r2} \ \sigma_2 \ \epsilon_{r3} \ \sigma_3]^T$ . The results obtained using our approach have a very good agreement with those obtained using CFD technique. As an example, the sensitivities of the attenuation coefficient and phase constants of the fundamental TE mode with respect to  $\epsilon_{r3}$  are shown in Figs. 10 and 11, respectively. The CFD approach requires 24 additional simulations to obtain the sensitivity with respect to all the design parameters. On the other hand, our approach requires no additional simulation.

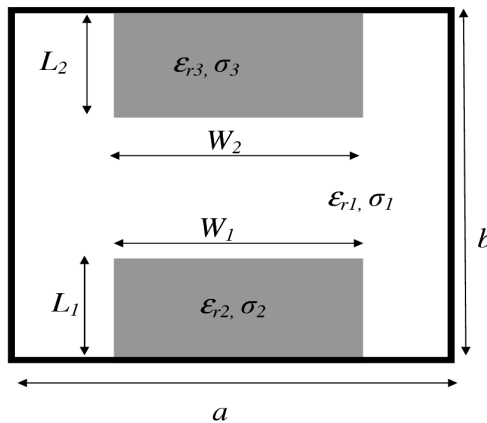


**Figure 7.** Schematic diagram of the double post loaded dielectric waveguide.

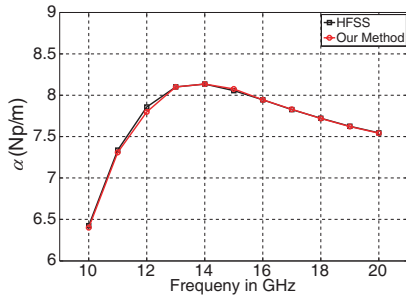


**Figure 8.** The attenuation coefficient of the dominant mode for the double post partially loaded waveguide.

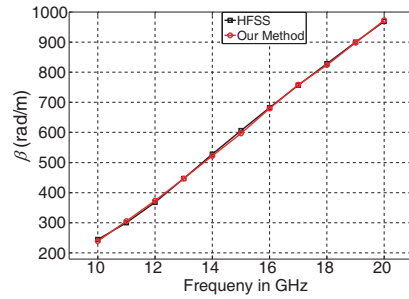


**Figure 9.** The phase constant of the dominant mode for the double post partially loaded waveguide.

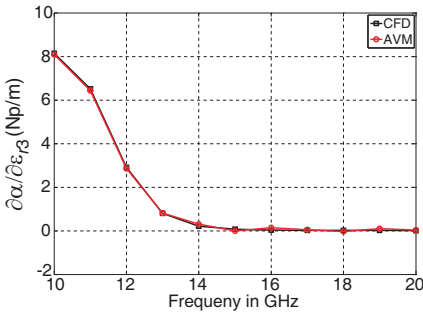


**Figure 10.** Sensitivity of the attenuation coefficients of the double posts partially loaded dielectric waveguide with respect to the permittivity  $\epsilon_{r3}$ .

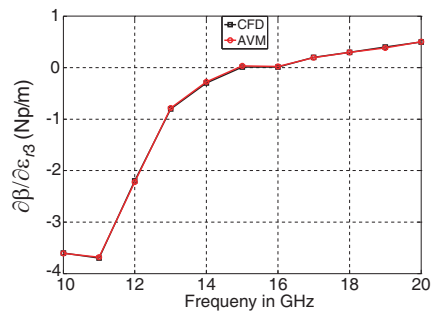


**Figure 11.** Sensitivity of the phase constant of the double posts partially loaded dielectric waveguide with respect to the permittivity  $\epsilon_{r3}$ .

### 5.3. W-Shape Leaky Waveguide

The third example is a W-shape leaky waveguide as shown in Fig. 12. For this structure, the fundamental mode has a complex propagation constant where the attenuation term is mainly affected by the design and material parameters [34]. The width of the main guiding region  $W_1$  and the cladding region  $W_2$  are taken to be  $1.014 \mu\text{m}$  and  $5.096 \mu\text{m}$ , respectively. The refractive indexes are  $n_1 = 1.45$  and  $n_2 = 1.39$ . The results obtained using our approach have a very good agreement with those reported in [34]. To further verify the results, a mode solver with PML included is developed as given in [35]. The results

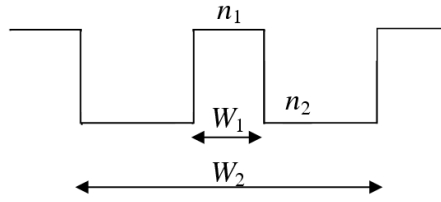


**Figure 12.** Refractive index distribution of W-shape leaky waveguide.

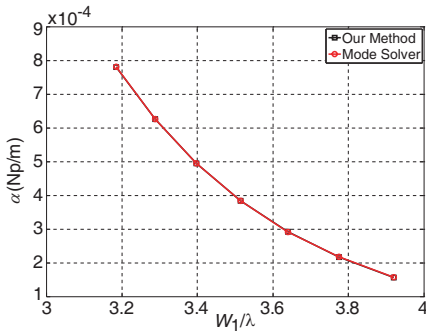


**Figure 13.** The attenuation coefficients of the W-shape leaky waveguide.

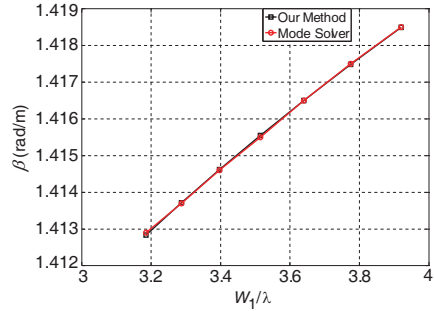


**Figure 14.** The phase constant of the W-shape leaky waveguide.

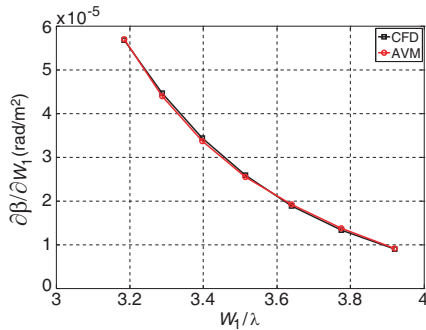


**Figure 15.** Sensitivity of the phase constant of the W-shape leaky waveguide with respect to  $W_1$ .

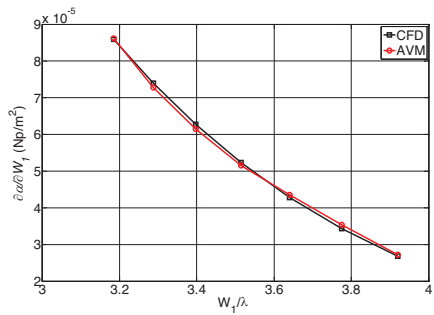


**Figure 16.** Sensitivity of the attenuation coefficients of the W-shape leaky waveguide with respect to  $W_1$ .

using our approach have very good agreement with those obtained using the mode solver with PML as shown in Figs. 13 and 14. The vector of design parameters in this example is  $\mathbf{p} = [W_1 W_2 n_1 n_2]^T$ . The obtained results have good agreement with those obtained using the CFD technique applied directly at the level of response. For illustration, the sensitivity of the phase and attenuation terms of the propagation constants with respect to the variation in  $W_1$  is shown in Figs. 15 and 16, respectively.

## 6. CONCLUSION

We propose an efficient approach to extract the modal parameters and their sensitivities with respect to all the design parameters. Our approach is general and can be utilized for lossless, lossy, and leaky structures. The exploitation of the adopted MPM allows for significant reduction in the computational time and memory requirements. Our technique requires no extra simulation for extracting the modal parameters and their sensitivities with respect to all the design parameters over the whole band of frequencies. The efficiency and versatility of our technique have been shown through different examples.

## REFERENCES

1. Young, G. O. and R. Vahldieck, "An efficient 2D FDTD algorithm using real variables," *IEEE Microwave Guided Wave Lett.*, Vol. 3, May 1993.
2. Jin, H. and R. Vahldieck, "Full-wave analysis of guiding structures using a 2-D array of 3-D TLM nodes," *IEEE Trans. Microw. Theory Tech.*, Vol. 41, 472–477, March 1993.
3. Xiao, J. K. and Y. Li, "Analysis for transmission characteristics of similar rectangular guide filled with arbitrarily-shaped inhomogeneous dielectric," *Journal of Electromagnetic Waves and Application*, Vol. 20, No. 3, 331–340, 2006.
4. Zhao, Y.-J., K.-L. Wu, and K.-K. M. Cheng, "A compact 2-D full-wave finite-difference frequency-domain method for general guided wave structures," *IEEE Trans. Microw. Theory Tech.*, Vol. 50, 1844–1848, July 2002.
5. Shahi, A. K., V. Singh, and S. P. Ojha, "Dispersion characteristics of electromagnetic waves in circularly cored highly birefringent waveguide having elliptical cladding," *Progress In Electromagnetics Research*, PIER 75, 51–62, 2007.

6. Pandey, P. C., A. Mishra, and S. P. Ojha, "Modal dispersion characteristics of a single mode dielectric optical waveguide with a guiding region cross-section bounded by two involuted spirals," *Progress In Electromagnetics Research*, PIER 73, 1–13, 2007.
7. Dydyk, M., "Microstrip directional couplers with ideal performance via single-element compensation," *IEEE Trans. Microw. Theory Tech.*, Vol. 47, No. 6, 956–964, 1999.
8. Swillam, M. A., M. H. Bakr, and X. Li, "Design optimization of compact wideband optical switch exploiting stair case index MMI," *IEEE J. Lightwave Technology*, Vol. 27, 80–87, January 2009.
9. Huang, W. P. and C. L. Xu, "Simulation of three-dimensional optical waveguides by a full-vector beam propagation method," *IEEE J. Quantum Electron.*, Vol. 29, 2639–2649, October 1993.
10. Mansour, R. R. and R. H. MacPhie, "An improved transmission matrix formulation of cascaded discontinuities and its application to  $E$ -plane circuits," *IEEE Trans. Microw. Theory Tech.*, Vol. 34, 1490–1498, December 1986.
11. Swillam, M. A., M. H. Bakr, and X. Li, "Full wave sensitivity analysis of guided wave structures using FDTD," *Journal of Electromagnetic Waves and Application*, Vol. 22, No. 16, 2135–2145(11), 2008.
12. Nikolova, N. K., Y. Li, and M. H. Bakr, "Sensitivity analysis of scattering parameters with electromagnetic time-domain simulators," *IEEE Trans. Microw. Theory Tech.*, Vol. 54, 1598–1610, April 2006.
13. Swillam, M. A., M. H. Bakr, and X. Li, "Accurate sensitivity analysis of photonic devices exploiting the finite-difference time-domain central adjoint variable method," *J. Applied Optics*, Vol. 46, No. 9, 1492–1499, March 2007.
14. Swillam, M. A., M. H. Bakr, N. K. Nikolova, and X. Li, "Adjoint sensitivity analysis of dielectric discontinuities using FDTD," *Electromagnetics*, Vol. 27, No. 2, 123–140, February 2007.
15. Khajehpour, A. and S. A. Mirtaheri, "Analysis of pyramid EM wave absorber by fdtd method and comparing with capacitance and homogenization methods," *Progress In Electromagnetics Research Letters*, Vol. 3, 123–131, 2008.
16. Mohammad-Amjadi, S. and M. Soleimani, "Design of band-pass waveguide filter using frequency selective surfaces loaded with surface mount capacitors based on split-field update FDTD method," *Progress In Electromagnetics Research B*, Vol. 3, 271–281, 2008.

17. Ali, M. and S. Sanyal, "FDTD analysis of rectangular waveguide in receiving mode as EMI sensors," *Progress In Electromagnetics Research B*, Vol. 2, 291–303, 2008.
18. Lei, J.-Z., C.-H. Liang, W. Ding, and Y. Zhang, "EMC analysis of antennas mounted on electrically large platforms with parallel FDTD method," *Progress In Electromagnetics Research*, PIER 84, 205–220, 2008.
19. Jiang, Y.-N., D.-B. Ge, and S.-J. Ding, "Analysis of TF-SF boundary for 2D-FDTD with plane P-wave propagation in layered dispersive and lossy media," *Progress In Electromagnetics Research*, PIER 83, 157–172, 2008.
20. Liu, Y., Z. Liang, and Z. Yang, "Computation of electromagnetic dosimetry for human body using parallel FDTD algorithm combined with interpolation technique," *Progress In Electromagnetics Research*, PIER 82, 95–107, 2008.
21. Wang, M. Y., J. Xu, J. Wu, B. Wei, H.-L. Li, T. Xu, and D.-B. Ge, "FDTD study on wave propagation in layered structures with biaxial anisotropic metamaterials," *Progress In Electromagnetics Research*, PIER 81, 253–265, 2008.
22. Afrooz, K., A. Abdipour, A. Tavakoli, and M. Movahhedi, "Time domain analysis of active transmission line using FDTD technique (application to microwave/MM-wave transistors)," *Progress In Electromagnetics Research*, PIER 77, 309–328, 2007.
23. Xiao, S.-Q., B.-Z. Wang, P. Du, and Z. Shao, "An enhanced FDTD model for complex lumped circuits," *Progress In Electromagnetics Research*, PIER 76, 485–495, 2007.
24. Hadi, M. F. and S. F. Mahmoud, "Optimizing the compact-FDTD algorithm for electrically large waveguiding structures," *Progress In Electromagnetics Research*, PIER 75, 253–269, 2007.
25. Ali, M. and S. Sanyal, "FDTD analysis of dipole antenna as EMI sensor," *Progress In Electromagnetics Research*, PIER 69, 341–359, 2007.
26. Gong, Z. and G.-Q. Zhu, "FDTD analysis of an anisotropically coated missile," *Progress In Electromagnetics Research*, PIER 64, 69–80, 2006.
27. Feit, M. D. and J. A. Jr Fleck, "Computation of mode properties in optical fiber waveguides by a propagation beam method," *J. Applied Optics*, Vol. 19, 1154–1164, April 1980.
28. Ko, W. L. and R. Mittra, "A combination of FD-TD and Prony's method for analyzing microwave integrated circuits," *IEEE Trans. Microw. Theory Tech.*, Vol. 39, 2176–2181, 1991.

29. Sarkar, T. K. and O. Pereira, "Using the matrix pencil method to estimate the parameters of a sum of complex exponentials," *IEEE Antennas Propagat. Mag.*, Vol. 37, 48–55, February 1995.
30. Feng, N. N., G. R. Zhou, and W. P. Huang, "Mode calculation by beam propagation method combined with digital signal processing technique," *IEEE J. Quantum Electron.*, Vol. 39, 1111–1117, September 2003.
31. Cover, T. M. and J. A. Thomas, *Elements of Information Theory*, John Wiley, 1991.
32. Sacks, Z. S., D. M. Kingsland, R. Lee, and J. F. Lee, "A perfectly matched anisotropic absorber for use as an absorbing boundary condition," *IEEE Trans. Antennas Propagat.*, Vol. 43, 1460–1463, December 1995.
33. Ansoft, available at <http://www.ansoft.com/products/hf/hfss/>.
34. Hu, J. and C. R. Menyuk, "Understanding leaky modes: Slab waveguide revisited," *Adv. Opt. Photon.*, Vol. 1, 58–106, 2009.
35. Huang, W.-P., C.-L. Xu, W. Lui, and K. Yokoyama, "The perfectly matched layer boundary condition for modal analysis of optical waveguides: Leaky mode calculations," *IEEE Photon. Technol. Lett.*, Vol. 8, No. 5, 652–654, 1996.